The international journal of science / 9 November 2023

nature

index
Rising stars

SOCIAL BONDS

Shifting priorities prompt dynamic retuning of dopamine reward system in zebra finch brains

Author choice
Plan S group seeks radical revolution in science publishing

Mind machine
Could AI help to unpick the complexities of the human brain?

Integrity check
Refined predictions for the stability of crystal structures

Vol. 623, No. 7986
nature.com

Article

Dopaminergic error signals retune to social feedback during courtship

https://doi.org/10.1038/s41586-023-06580-w

Received: 23 February 2019

Accepted: 30 August 2023

Published online: 27 September 2023

Check for updates

Andrea Roeser[1,3], Vikram Gadagkar[1,2,3]✉, Anindita Das[1], Pavel A. Puzerey[1], Brian Kardon[1] & Jesse H. Goldberg[1]✉

Hunger, thirst, loneliness and ambition determine the reward value of food, water, social interaction and performance outcome[1]. Dopamine neurons respond to rewards meeting these diverse needs[2–8], but it remains unclear how behaviour and dopamine signals change as priorities change with new opportunities in the environment. One possibility is that dopamine signals for distinct drives are routed to distinct dopamine pathways[9,10]. Another possibility is that dopamine signals in a given pathway are dynamically tuned to rewards set by the current priority. Here we used electrophysiology and fibre photometry to test how dopamine signals associated with quenching thirst, singing a good song and courting a mate change as male zebra finches (*Taeniopygia guttata*) were provided with opportunities to retrieve water, evaluate song performance or court a female. When alone, water reward signals were observed in two mesostriatal pathways but singing-related performance error signals were routed to Area X, a striatal nucleus specialized for singing. When courting a female, water seeking was reduced and dopamine responses to both water and song performance outcomes diminished. Instead, dopamine signals in Area X were driven by female calls timed with the courtship song. Thus the dopamine system handled coexisting drives by routing vocal performance and social feedback signals to a striatal area for communication and by flexibly re-tuning to rewards set by the prioritized drive.

Motivated behaviours are organized around objectives defined by an animal's need[1]. For example, thirsty or hungry animals approach and learn from water- or food-predicting cues, in part due to reward prediction error (RPE) signalling by mesostriatal dopamine neurons[2,3]. Dopamine prediction error signals have also been observed in response to social and motor performance outcomes, supporting the generality of dopamine reinforcement mechanisms across a wide range of behaviours[4–8]; yet it remains unclear how phasic dopamine signals can evaluate outcomes in complex and natural conditions where an animal may weigh multiple objectives at once[9,11]. For instance, it is unknown how an animal that is thirsty, sexually motivated and actively practicing motor performance weighs its responses. One possible solution is that brainwide signals, including mesostriatal dopamine responses, are dynamically modulated according to current priorities[12]. For example, dopamine responses to water cues would retune to social outcomes if an animal prioritizes courtship over thirst. A mutually inclusive possibility is that different mesostriatal dopamine pathways are anatomically segregated to signal outcomes according to distinct objectives[9,10,13]. This idea would predict that dopamine responses to social outcomes would not be globally broadcast[14–16], but instead specifically routed to striatal areas dedicated to social communication.

To test whether dopamine signals are dynamically modulated by changing priorities, we examined dopamine responses to water rewards, song errors and social interactions. Concurrently, to test whether dopamine signals associated with different objectives are globally broadcast[14–16] or anatomically routed to unique striatal regions[9,10,13], we measured dopamine release in two distinct striatal areas: Area X, the striatal region of a nucleated circuit called the song system[17,18], and a medial striatal area (MST) that lacks connectivity with the nucleated song system and that arises from a separate group of dopamine neurons in the ventral tegmental area (VTA)[17–20] (Extended Data Fig. 1).

Courtship reduces dopamine responses to water cues

We first examined behavioural and dopaminergic responses to water rewards. Water-deprived zebra finches were trained to peck, within 8 s of a 'reward' light cue, a touch-sensing spout that dispensed water with a probability of 70% (Methods). Birds also learned to ignore a different colour 'no-reward' light cue unassociated with water (retrieval rate following reward and no-reward light cues in lone, not-singing birds: 78.1 ± 11.4% and 3.8 ± 2.1%, respectively, $n = 13$ birds; Fig. 1a–c). We used genetically encoded dopamine sensors and fibre photometry to measure dopamine release in Area X ($n = 9$ hemispheres, 7 birds) or MST ($n = 9$ hemispheres, 6 birds) (Fig. 1d and Methods). Both Area X and MST exhibited significantly larger activations of dopamine release following rewarded versus unrewarded spout contacts, consistent with classic RPE signalling[2,3] (Extended Data Fig. 2).

To test whether the water retrieval depended on singing or female interaction, we presented light cues to thirsty birds under four conditions: when they were alone and not singing, alone and singing, with

[1]Department of Neurobiology and Behavior, Cornell University, Ithaca, NY, USA. [2]Department of Neuroscience, Zuckerman Mind Brain Behavior Institute, Columbia University, New York, NY, USA. [3]These authors contributed equally: Andrea Roeser, Vikram Gadagkar. ✉e-mail: vikram.gadagkar@columbia.edu; jessehgoldberg@gmail.com

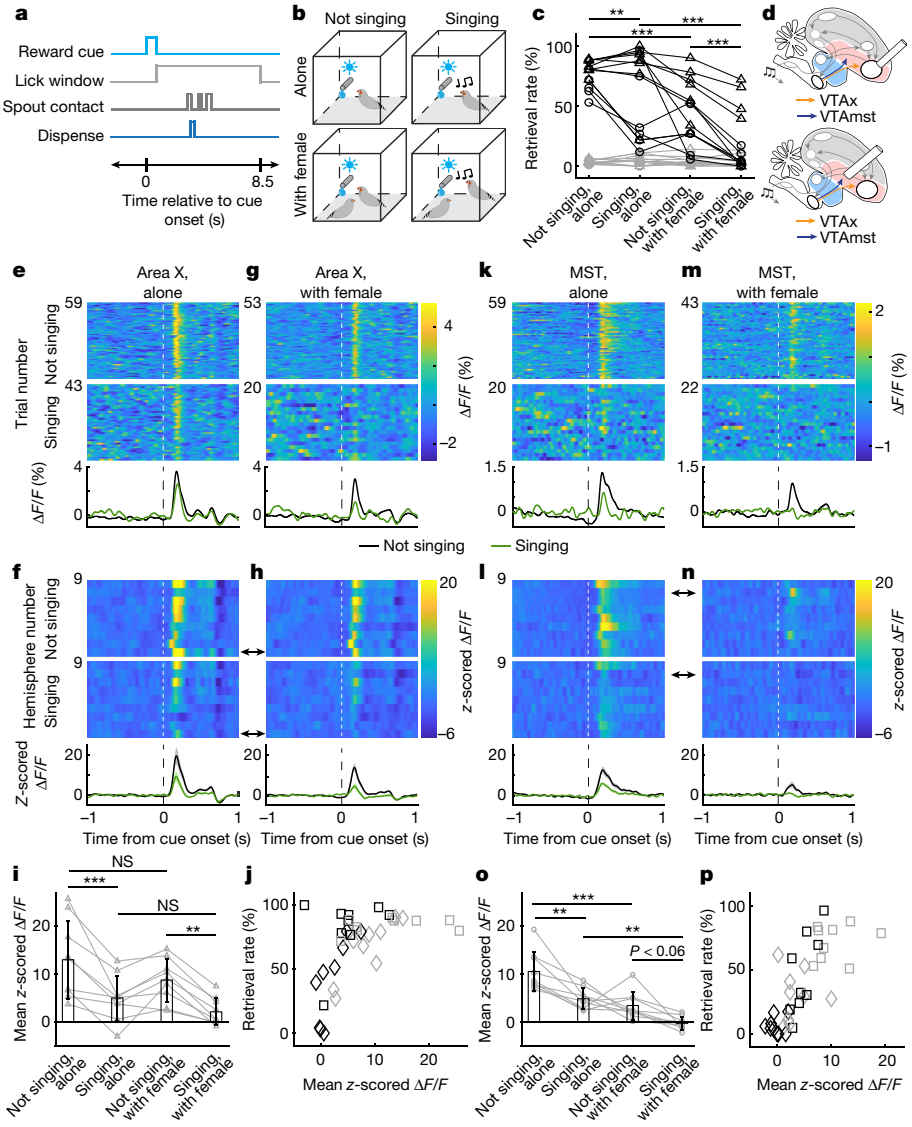

Fig. 1 | Courtship reduces behavioural and dopaminergic responses to water cues in water-deprived zebra finches. a, Example trial in which a 'reward' light cues water availability from a touch-sensing spout. **b**, Water availability under four behavioural conditions. **c**, Water retrieval probability for reward (black) and no-reward (grey) light cues across behavioural conditions (Area X-implanted bird, triangles, $n = 7$ birds; MST-implanted bird, circles, $n = 6$ birds; not singing, alone versus singing, alone: $P = 0.0033$; not singing, alone versus not singing, with female: $P = 1.9 \times 10^{-16}$; singing, alone versus singing with female: $P = 1.9 \times 10^{-17}$; not singing, with female versus singing, with female: $P = 1.0 \times 10^{-10}$; generalized linear mixed effects model with post hoc contrast tests; Methods). **d**, Brain diagrams indicating recording sites (top, Area X; bottom, MST). **e**,**f**, Dopamine responses in Area X when the bird was alone. **e**, Single-trial dopamine responses to the reward light cue from a single Area X hemisphere during not singing (top) or singing (bottom) conditions. **f**, Average z-scored $\Delta F/F$ responses to reward light cue across 9 Area X hemispheres (top). Data are mean ± s.e.m. z-scored $\Delta F/F$ across hemispheres (bottom). Black arrow denotes response from the example hemisphere in **e**. **g**,**h**, Data plotted as in **e**,**f**, with female present. **i**, Average values across all Area X hemispheres (mean ± s.d., black bars) and mean z-scored values for each hemisphere ($n = 9$ hemispheres; grey dots joined with lines) for the four behavioural conditions in **e**–**h** (not singing, alone versus singing, alone: $P = 0.00025$; not singing, alone versus not singing, with female: $P = 0.067$; singing, alone versus singing, with female: $P = 0.32$; not singing, with female versus singing, with female: $P = 0.0022$; 2-way ANOVA and post hoc Tukey test; Methods). **j**, Retrieval rate in each behavioural condition plotted against the Area X dopamine response from that condition (black, singing; grey, not singing; square, alone; diamond, with female; $R^2 = 0.28$ and $P = 9.3 \times 10^{-4}$). **k**–**p**, Data plotted as in **e**–**j** for dopamine recordings in MST ($n = 9$ hemispheres). **o**, Average values across all hemispheres (mean ± s.d., black bars) and mean z-scored values for each hemisphere ($n = 9$ hemispheres; grey dots joined with lines) for the 4 behavioural conditions in **k**–**n** (not singing, alone versus singing, alone: $P = 0.0013$; not singing, alone versus not singing, with female: $P = 8.3 \times 10^{-5}$; singing, alone versus singing, with female: $P = 0.0044$; not singing, with female versus singing, with female: $P = 0.056$; 2-way ANOVA and post hoc Tukey test; Methods). **p**, $R^2 = 0.54$ and $P = 2.9 \times 10^{-7}$. All P values equal or smaller than 0.06 are indicated on the figure; $n = 9$ Area X and $n = 9$ MST hemispheres. Note that data in **c** and **j**,**p** do not align because data in **c** are plotted by bird whereas those in **j**,**p** are plotted by hemisphere (Methods). $^*P < 0.05$, $^{**}P < 0.01$, $^{***}P < 0.001$. NS, not significant.

the female and not singing, and with the female and actively singing courtship song (Fig. 1b and Methods). Birds were most likely to retrieve water when alone and not singing, significantly less likely when singing alone, and least likely when singing to a female (Fig. 1c). Birds were most likely to ignore the water cues while singing to a female, suggesting that courtship reduced the expression of thirst.

We next measured dopamine responses to light cues in Area X and MST across these four behavioural conditions. Cue-evoked dopamine

release was similarly robust and reliable in both Area X and MST when birds were alone and not singing (Fig. 1e,f,k,l, black), consistent with widespread responses to water-predicting cues in mammals[3]. Cue-evoked dopamine signals in both regions were significantly reduced when the male was singing alone (Fig. 1e,f,k,l, green), and reduced even further when singing to a female (Fig. 1g,h,l,m,n,o). Thus, courtship also reduced dopamine responses to water cues, consistent with the decreased water-seeking behaviour in the presence of the female.

To test how phasic dopamine signals correlated with water seeking, we plotted cue-evoked dopamine responses against the water retrieval probability within each behavioural condition ($n = 9$ MST hemispheres; $n = 9$ Area X hemispheres). In both Area X and MST, the magnitude of dopamine response was strongly correlated with retrieval probability (Fig. 1j,p), revealing a strong relationship between dopamine responses to water cues and water-seeking behaviour. Yet notably, dopamine responses to no-reward light cues also strongly diminished during both lone and courtship singing even though retrieval rates were always low, demonstrating that the modulation of dopamine signals by behavioural condition can be decoupled from behavioural response (Extended Data Fig. 3). Although MST-implanted birds were less likely to retrieve water across some conditions (Fig. 1c), water cue signals and their relationship with retrieval were similar in both MST and Area X (Fig. 1j,p). Together, these data show that the act of singing, especially to a female, reduces water seeking as well as dopamine responses to reward-predicting cues.

Singing-related error signals are routed to Area X

We next explored first whether singing-related dopamine signals were routed to distinct striatal areas and second, whether they depended on courtship state. When alone, zebra finches spontaneously engage in bouts of singing, and their objective is to learn or maintain a song that matches the memory of a tutor song heard early in life[21–23]. Introduction of a female induces an immediate transition to a courtship state characterized by pursuit behaviour and female-directed song[21,24]. Past electrophysiological recordings from Area X-projecting VTA neurons (VTAx neurons) in males singing alone discovered dopaminergic performance error signals: phasic activations in dopamine spiking followed better-than-predicted song outcomes, and phasic suppressions followed unexpected errors[8,25]. To test whether these singing-related error signals are specifically routed to the song system, we measured dopamine release in Area X or MST in birds singing alone (Area X: $n = 19$ hemispheres, 14 birds; MST: $n = 9$ hemispheres, 6 birds). Perceived song errors were controlled with distorted auditory feedback (DAF), a 50-ms-duration song-like sound played probabilistically on top of a specific target syllable in the bird's song[8,24,26–28] (Methods and Supplementary Information). In Area X, phasic suppressions of dopamine release followed DAF and phasic activations followed undistorted target syllable renditions at the precise moment that DAF would have occurred but did not (Fig. 2a,b), consistent with past electrophysiological recordings from VTAx neurons in lone males[8]. To quantify error responses, we compared the average dopamine fluorescence between distorted and undistorted songs in the 0.15–0.3 s interval following target onset (target onset is defined as the median DAF onset time relative to distorted syllable onset; Methods). We defined the error score as the z-scored difference between target onset-aligned distorted and undistorted fluorescence[8,29], and found significant error signalling in all Area X hemispheres (error score >2 in 19 out of 19 hemispheres, mean error score 7.4 ± 2.9; Fig. 2g). By contrast, singing-related error signals were rarely observed in MST (error score >2 in 2 out of 9 hemispheres; mean error score: 0.8 ± 1.8; Fig. 2g). To our knowledge, this is the first demonstration that dopamine performance error signals are routed to the specific part of the motor system producing the evaluated behaviour.

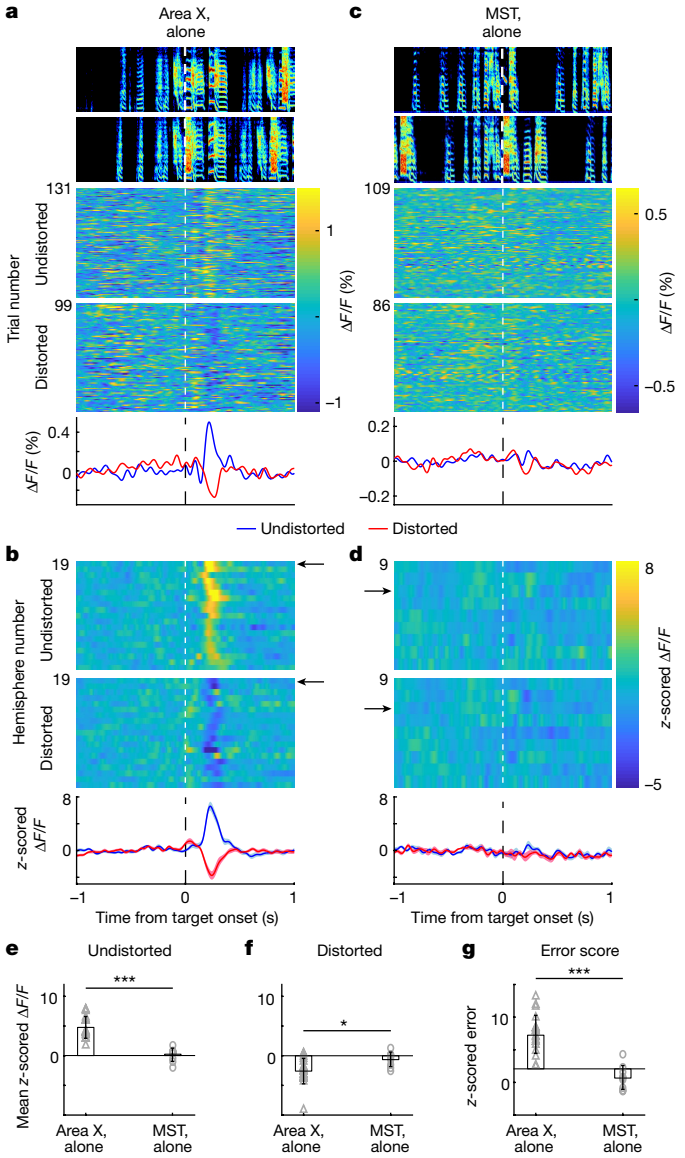

Fig. 2 | Singing-related error signals are routed to Area X and not MST in birds singing alone. a, Spectrograms and single-trial dopamine responses for undistorted (top) and distorted (bottom) renditions recorded in a single Area X hemisphere of a bird singing alone, plotted above average $\Delta F/F$ signals (all plots aligned to target onset; blue: undistorted; red: distorted). **b**, z-Scored average from 19 Area X hemispheres aligned to undistorted (top) and distorted (bottom) renditions, black arrow indicates example hemisphere shown in **a**. Bottom, average z-scored response (mean ± s.e.m.). **c**,**d**, Data plotted as in **a**,**b** for signals recorded in 9 MST hemispheres. **e**,**f**, Mean z-scored $\Delta F/F$ value for each hemisphere (grey dots) in the 150–300 ms window following undistorted (**e**; $P = 3.6 \times 10^{-5}$; unpaired, two-sided Wilcoxon rank sum test) and distorted (**f**; $P = 0.012$; unpaired, two-sided Wilcoxon rank sum test) renditions in Area X ($n = 19$ hemispheres; triangles) versus MST ($n = 9$ hemispheres; circles). Black bars, mean ± s.d. across all hemispheres. **g**, z-Scored error responses in Area X and MST for each hemisphere (Area X: $n = 19$ hemispheres; MST: $n = 9$ hemispheres; grey dots) and across hemispheres (mean ± s.d., black bars; $P = 5.5 \times 10^{-5}$; unpaired, two-sided Wilcoxon rank sum test). Spectrograms in **a** and **c** (and all further instances) range from 0.5–7.5 kHz.

Courtship reduces singing-related error signals

We next investigated whether performance error signals in the VTAx pathway depended on courtship state in the same way as the water-reward signals. If self-evaluation remains the goal during

courtship singing, then error signals in the VTAx pathway might be similar whether the female is present or absent. Alternatively, if the bird's objective changes, for example away from song evaluation and towards eliciting responses in the female, then dopamine signals may retune to respond to affiliative female behaviours. To test these possibilities, we measured dopamine responses to DAF-induced performance errors when birds sang alone and to females (Methods). Error signals that were robust in Area X when the male sang alone were reduced or eliminated during courtship singing[24] (per cent reduction in phasic activations: 64.4 ± 21.1%, $n = 19$ hemispheres; per cent reduction in phasic suppressions: 27.0 ± 74.7%, $n = 19$ hemispheres; mean error score, alone = 7.4 ± 2.9 versus with female = 3.4 ± 2.5, Fig. 3). To test whether this modulation of dopamine release in Area X also occurred in the spiking of VTAx dopamine neurons[30], we carried out electrophysiological recordings from antidromically identified Area X-projecting VTA neurons in singing birds hearing syllable-targeted DAF. We observed a similar courtship-associated reduction of performance error signals at the level of dopamine spikes (Extended Data Fig. 4 and Methods). Again consistent with the anatomical routing of singing-related error signals, dopamine release in MST remained unresponsive to DAF during courtship singing (Extended Data Fig. 5).

We also noted that baseline levels of dopamine in Area X increased during both alone and female-directed singing (Extended Data Fig. 6a–f), but this increase was not observed in the spiking of VTAx neurons (Extended Data Fig. 6m–r). Further, although the cued moment of female arrival drove phasic dopamine release, especially in MST (Extended Data Fig. 7e and Methods), baseline striatal dopamine levels did not increase with courtship state (Extended Data Fig. 7a–d,f), consistent with the idea that noradrenergic inputs to Area X and other parts of the song system may influence courtship singing and behaviour[31]. Baseline discharge of VTAx neurons during not-singing periods was subtly affected by courtship context (Extended Data Fig. 8i,j). Note that although our study focuses on mesostriatal dopamine projections, a different dopamine projection to the premotor nucleus HVC of the song system is also associated with courtship singing and may exhibit different functions and signals[32,33].

Dopamine signals retune to social feedback

We hypothesized that modulation of dopaminergic reward and performance evaluation signals during courtship allows the mesostriatal systems to retune to outcomes associated with a new objective, such as eliciting positive social feedback from the female. In zebra finches, calls provide affiliative feedback that supports bonding and reinforcement[21,34], suggesting that they may influence dopamine signals[35]. We aligned dopamine responses to natural female calls produced in two distinct phases of the courtship interaction: during periods when the male was not singing, and those produced during the male's song (Fig. 4). Female calls produced when the male was not singing evoked small and unreliable dopamine release in MST (mean z-scored response: 1.7 ± 1.7) and Area X (mean z-scored response: 1.9 ± 2.3). By contrast, female calls produced during the male's song drove marked and reliable dopamine release, but primarily in Area X (Area X mean z-scored response: 4.5 ± 2.4; MST mean z-scored response: 1.9 ± 1.4; Fig. 4). To control for the possibility that any unexpected external sound during courtship song could drive dopamine signals, we played the sounds of knocks, DAF or pre-recorded female calls throughout the courtship interaction (Methods). None of these stimuli drove reliable dopamine transients during singing (Fig. 4g and Extended Data Fig. 9). Thus only natural female calls in sync with the male song evoked dopamine release and specifically in Area X. To our knowledge, this is the first demonstration that a temporally coordinated social interaction drives a phasic

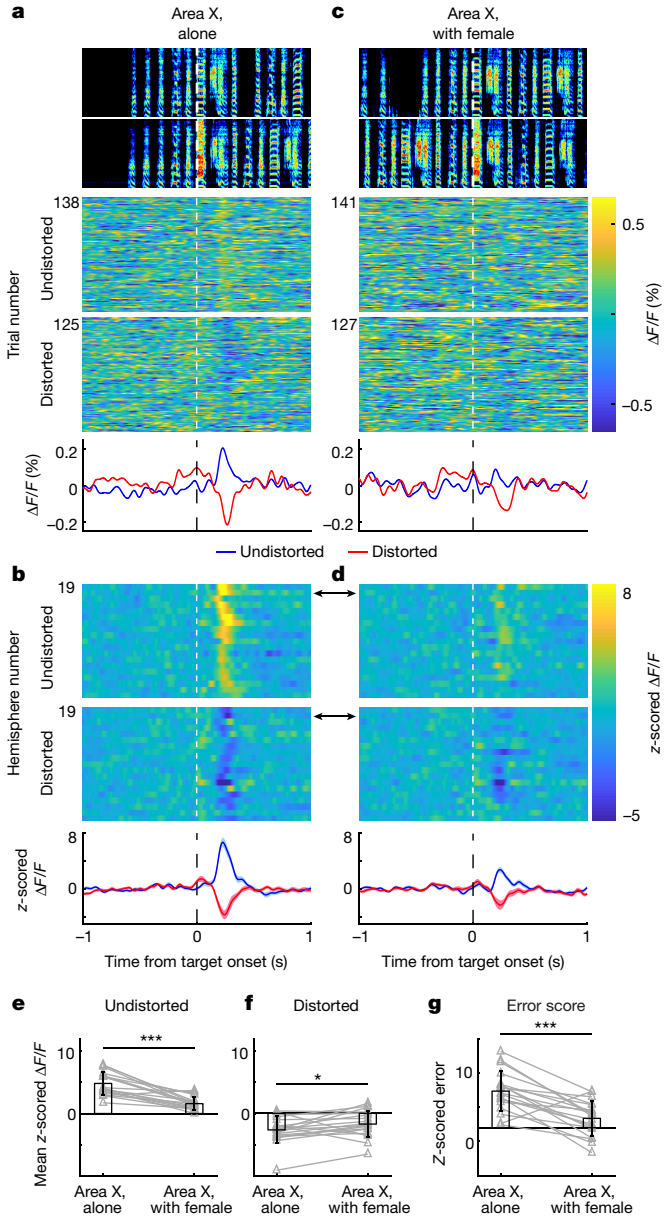

Fig. 3 | Singing-related error signals in Area X are reduced during courtship singing. a, Spectrograms and single-trial dopamine responses for undistorted (top) and distorted (bottom) renditions recorded in a single Area X hemisphere of a bird singing alone, plotted above average ΔF/F signals (different example hemisphere from Fig. 2a; plots aligned to target onset; blue: undistorted; red: distorted). **b**, z-Scored average from 19 Area X hemispheres aligned to undistorted (top) and distorted (bottom) renditions, black arrow indicates example hemisphere shown in **a**; bottom: average z-scored response (mean ± s.e.m.). **c**, Data plotted as in **a** for the same hemisphere measured during courtship singing. **d**, Data plotted as in **b** for the same hemispheres recorded during courtship singing. **e**,**f**, Scatter plots of average across all hemispheres (mean ± s.d., black bars) and mean z-scored ΔF/F value for each hemisphere (grey dots joined with lines; $n = 19$ hemispheres) in the 150–300 ms following undistorted (**e**; $P = 5.5 \times 10^{-6}$; 2-way ANOVA and post hoc Tukey test; Methods) and distorted (**f**; $P = 0.037$; 2-way ANOVA and post hoc Tukey test; Methods) renditions in Area X during alone versus female-directed singing. **g**, Scatter plots of mean z-scored error for each hemisphere (grey dots joined with lines; $n = 19$ hemispheres) and average z-scored error responses across hemispheres (mean ± s.d., black; $P = 8.4 \times 10^{-4}$; paired, two-sided Wilcoxon signed rank test) when birds sang alone versus to females.

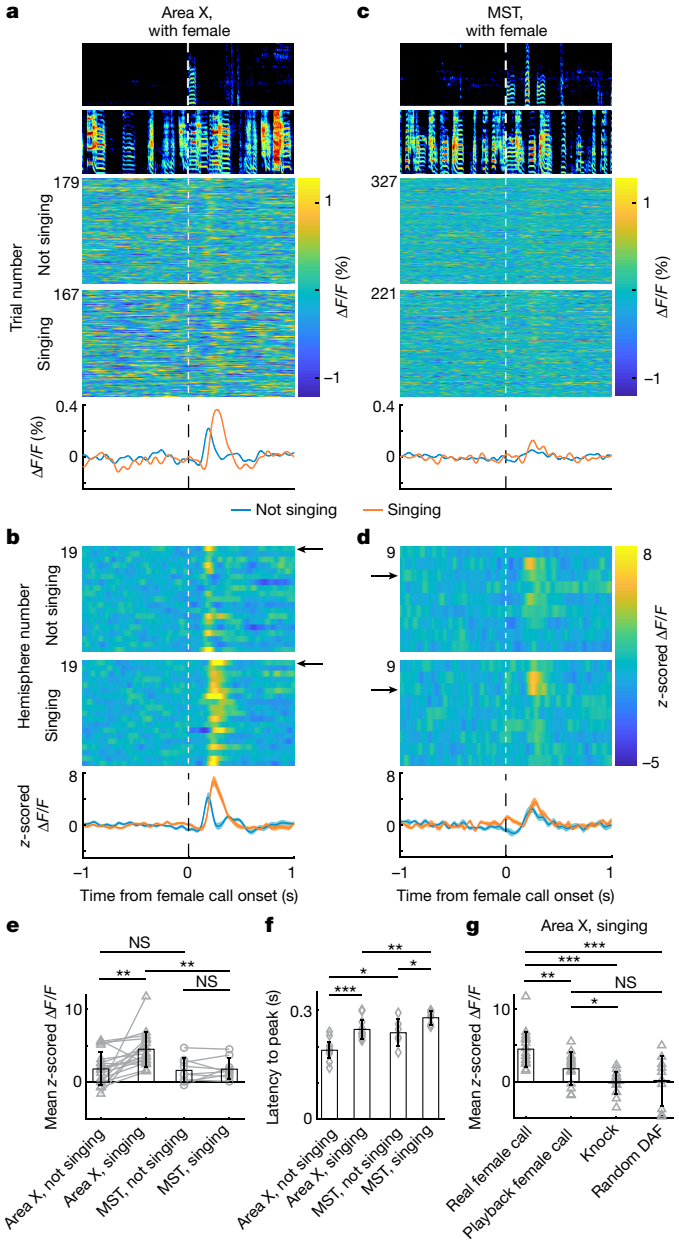

Fig. 4 | Female calls timed with male courtship singing drive phasic dopamine activations in Area X. a, Spectrograms and single-trial Area X dopamine responses to natural female calls during not singing (top) or singing (bottom) periods of the courtship interaction, plotted above average $\Delta F/F$ signals (plots aligned to onset of female call). **b**, *z*-Scored average from 19 Area X hemispheres, black arrow indicates example hemisphere shown in **a**; bottom: average *z*-scored response (mean ± s.e.m.). **c**,**d**, Data plotted as in **a**,**b** for dopamine signals recorded in MST. **e**, Scatter plots of mean *z*-scored $\Delta F/F$ across all hemispheres (mean ± s.d., black bars) and for each hemisphere (grey dots joined with lines; $n = 19$ Area X hemispheres and $n = 9$ hemispheres in MST) in the 150–300 ms window following female call onset produced during singing or not singing periods (triangles: Area X; circles: MST; Area X, not singing versus Area X singing: $P = 0.0015$; MST, not singing versus MST, singing: $P = 0.73$; paired, two-sided Wilcoxon signed rank test; Area X, not singing versus MST, not singing: $P = 0.96$; Area X, singing versus MST, singing: $P = 0.0023$; unpaired, two-sided Wilcoxon rank sum test). **f**, Latency to peak *z*-scored response in a 300 ms window following real female calls during singing or not singing in Area X and MST as an average across all hemispheres (mean ± s.d., black bars) and single hemispheres (grey dots; only responses that were greater than a *z*-score value of 2 within the window were included; Area X, not singing: $n = 17$; Area X, singing: $n = 19$; MST, not singing: $n = 6$; MST, singing: $n = 8$; Area X, not singing versus Area X singing: $P = 4.3 \times 10^{-6}$; MST, not singing versus MST, singing: $P = 0.043$; Area X, not singing versus MST, not singing: $P = 0.016$; Area X, singing versus MST, singing: $P = 0.0078$; unpaired, two-sided Wilcoxon rank sum test). **g**, *z*-Scored magnitudes of dopamine responses in Area X to real female calls ($n = 19$ hemispheres) compared to playbacks of a female call ($n = 14$ hemispheres), knock sounds ($n = 15$ hemispheres) and random DAF sounds ($n = 10$ hemispheres) played through speakers next to the bird during courtship singing (mean ± s.d., black bars; single hemispheres, grey dots; real call versus playback call: $P = 0.0038$; real call versus knock: $P = 1.7 \times 10^{-6}$; real call versus random DAF: $P = 0.0010$; playback call versus knock: $P = 0.017$; playback call versus random DAF: $P = 0.21$; unpaired, two-sided Wilcoxon rank sum test).

dopamine response specifically in a mesostriatal pathway dedicated to social communication.

Diverse ascending dopamine pathways are implicated in many functions, including movement vigour, mood, incentive salience and reward[36,37]. Here we focused specifically on how phasic mesostriatal dopamine signals, previously associated with reinforcement learning, depend on an animal's objective. A foundational premise of reinforcement learning is that animals learn to maximize future rewards[16], but what an animal finds rewarding will depend on its current priorities. Indeed, recent studies showing dopamine responses to food and water rewards as well as social and motor performance outcomes support the generality of mechanisms of reinforcement learning[2–8], but also raise the question of how dopamine responses can evaluate diverse outcomes as objectives change in natural, complex conditions where multiple drives may co-exist[11]. We discovered the dopamine system handles this problem in two ways. First, anatomically distinct mesostriatal dopamine pathways carried different signals: water reward signals were broadcast to both striatal regions, but dopamine responses to song performance and social outcomes were routed specifically to a pathway dedicated to social communication. Second, dopamine signals retuned according to the current objective: both reward- and song performance-related dopamine signals were reduced during courtship and were instead driven by female calls timed with male song. These results suggest that the bird's evaluation system prioritizes social feedback during courtship above other objectives. The neural mechanisms by which dopamine neurons change their tuning remain unclear. One possibility is that the hypothalamus and other ascending modulatory systems establish an animal's priorities that tune brainwide responses to relevant stimuli[12,31,38], including cortical responses to auditory feedback during singing[24]. It will be interesting to determine in future studies how social dopamine signals during courtship are prioritized and how they influence future interactions, pair formation and mating success.

Online content

Any methods, additional references, Nature Portfolio reporting summaries, source data, extended data, supplementary information, acknowledgements, peer review information; details of author contributions and competing interests; and statements of data and code availability are available at https://doi.org/10.1038/s41586-023-06580-w.

1. Maslow, A. H. A theory of human motivation. *Psychol. Rev.* **50**, 370 (1943).
2. Schultz, W. Behavioral dopamine signals. *Trends Neurosci.* **30**, 203–210 (2007).
3. Tsutsui-Kimura, I. et al. Distinct temporal difference error signals in dopamine axons in three regions of the striatum in a decision-making task. *eLife* **9**, e62390 (2020).
4. Solié, C., Girard, B., Righetti, B., Tapparel, M. & Bellone, C. VTA dopamine neuron activity encodes social interaction and promotes reinforcement learning through social prediction error. *Nat. Neurosci.* **25**, 86–97 (2022).
5. Hu, R. K. et al. An amygdala-to-hypothalamus circuit for social reward. *Nat. Neurosci.* **24**, 831–842 (2021).
6. Dai, B. et al. Responses and functions of dopamine in nucleus accumbens core during social behaviors. *Cell Rep.* **40**, 111246 (2022).
7. Xie, Y., Huang, L., Corona, A., Pagliaro, A. H. & Shea, S. D. A dopaminergic reward prediction error signal shapes maternal behavior in mice. *Neuron* **111**, 557–570 (2023).

8. Gadagkar, V. et al. Dopamine neurons encode performance error in singing birds. *Science* **354**, 1278–1282 (2016).
9. Lee, R. S., Engelhard, B., Witten, I. B. & Daw, N. D. A vector reward prediction error model explains dopaminergic heterogeneity. Preprint at *bioRxiv* https://doi.org/10.1101/2022.02.28.482379 (2022).
10. Menegas, W., Akiti, K., Amo, R., Uchida, N. & Watabe-Uchida, M. Dopamine neurons projecting to the posterior striatum reinforce avoidance of threatening stimuli. *Nat. Neurosci.* **21**, 1421–1430 (2018).
11. Skals, N., Anderson, P., Kanneworff, M., Löfstedt, C. & Surlykke, A. Her odours make him deaf: crossmodal modulation of olfaction and hearing in a male moth. *J. Exp. Biol.* **208**, 595–601 (2005).
12. Allen, W. E. et al. Thirst regulates motivated behavior through modulation of brainwide neural population dynamics. *Science* **364**, 253 (2019).
13. Lammel, S., Lim, B. K. & Malenka, R. C. Reward and aversion in a heterogeneous midbrain dopamine system. *Neuropharmacology* **76**, 351–359 (2014).
14. Schultz, W., Dayan, P. & Montague, P. R. A neural substrate of prediction and reward. *Science* **275**, 1593–1599 (1997).
15. Houk, J., Adams, J. & Barto, A. in *Models of Information Processing in the Basal Ganglia* (eds Houk, J. C., Davis, J. L. & Beiser, D. G.) 249–270 (MIT Press, 1995).
16. Sutton, R. S. & Barto, A. G. *Reinforcement Learning: An Introduction* (MIT Press, 1998).
17. Iyengar, S., Viswanathan, S. S. & Bottjer, S. W. Development of topography within song control circuitry of zebra finches during the sensitive period for song learning. *J. Neurosci.* **19**, 6037–6057 (1999).
18. Person, A. L., Gale, S. D., Farries, M. A. & Perkel, D. J. Organization of the songbird basal ganglia, including Area X. *J. Comp. Neurol.* **508**, 840–866 (2008).
19. Bottjer, S. W., Brady, J. D. & Cribbs, B. Connections of a motor cortical region in zebra finches: relation to pathways for vocal learning. *J. Comp. Neurol.* **420**, 244–260 (2000).
20. Karten, H. J. et al. Digital atlas of the zebra finch (*Taeniopygia guttata*) brain: a high-resolution photo atlas. *J. Comp. Neurol.* **521**, 3702–3715 (2013).
21. Zann, R. A. *The Zebra Finch: A Synthesis of Field and Laboratory Studies*, Vol. 5 (Oxford Univ. Press, 1996).
22. Theunissen, F. E. & Shaevitz, S. S. Auditory processing of vocal sounds in birds. *Curr. Opin. Neurobiol.* **16**, 400–407 (2006).
23. Woolley, S. C. & Woolley, S. M. in *The Neuroethology of Birdsong*, Vol. 71 (eds Sakata, J. et al.) 127–155 (2020).
24. Sakata, J. T. & Brainard, M. S. Social context rapidly modulates the influence of auditory feedback on avian vocal motor control. *J. Neurophysiol.* **102**, 2485–2497 (2009).
25. Duffy, A., Latimer, K. W., Goldberg, J. H., Fairhall, A. L. & Gadagkar, V. Dopamine neurons evaluate natural fluctuations in performance quality. *Cell Rep.* **38**, 110574 (2022).
26. Tumer, E. C. & Brainard, M. S. Performance variability enables adaptive plasticity of 'crystallized' adult birdsong. *Nature* **450**, 1240–1244 (2007).
27. Ali, F. et al. The basal ganglia is necessary for learning spectral, but not temporal, features of birdsong. *Neuron* **80**, 494–506 (2013).
28. Hoffmann, L. A., Saravanan, V., Wood, A. N., He, L. & Sober, S. J. Dopaminergic contributions to vocal learning. *J. Neurosci.* **36**, 2176–2189 (2016).
29. Chen, R. et al. Songbird ventral pallidum sends diverse performance error signals to dopaminergic midbrain. *Neuron* **103**, 266–276.e264 (2019).
30. Mohebi, A. et al. Dissociable dopamine dynamics for learning and motivation. *Nature* **570**, 65–70 (2019).
31. Singh Alvarado, J. et al. Neural dynamics underlying birdsong practice and performance. *Nature* **599**, 635–639 (2021).
32. Appeltants, D., Absil, P., Balthazart, J. & Ball, G. F. Identification of the origin of catecholaminergic inputs to HVc in canaries by retrograde tract tracing combined with tyrosine hydroxylase immunocytochemistry. *J. Chem. Neuroanat.* **18**, 117–133 (2000).
33. Ben-Tov, M., Duarte, F. & Mooney, R. A neural hub for holistic courtship displays. *Curr. Biol.* **33**, 1640–1653.e1645 (2023).
34. Hernandez, A. M., Perez, E. C., Mulard, H., Mathevon, N. & Vignal, C. Mate call as reward: acoustic communication signals can acquire positive reinforcing values during adulthood in female zebra finches (*Taeniopygia guttata*). *J. Comp. Psychol.* **130**, 36 (2016).
35. Tokarev, K. et al. Sexual dimorphism in striatal dopaminergic responses promotes monogamy in social songbirds. *eLife* **6**, e25819 (2017).
36. Schultz, W. Multiple dopamine functions at different time courses. *Annu Rev Neurosci* **30**, 259–288 (2007).
37. Smith, K. S., Berridge, K. C. & Aldridge, J. W. Disentangling pleasure from incentive salience and learning signals in brain reward circuitry. *Proc. Natl Acad. Sci. USA* **108**, E255–E264 (2011).
38. Riters, L. V. The role of motivation and reward neural systems in vocal communication in songbirds. *Front. Neuroendocrinol.* **33**, 194–209 (2012).

Methods

Animals

Subjects were 32 adult male zebra finches (*Taeniopygia guttata*, greater than 90 days old). All experiments were carried out in accordance with NIH guidelines and were approved by the Cornell Institutional Animal Care and Use Committee.

Surgery for photometry

Birds were anaesthetized with isoflurane and 1.25–1.75 µl of virus was injected either unilaterally or bilaterally into Area X (n = 12 right hemispheres; n = 7 left hemispheres; n = 14 birds) or MST (n = 3 right hemispheres; n = 6 left hemispheres; n = 6 birds) using a Nanoject II (Drummond Scientific) injector (one bird had a right hemisphere Area X implant and left hemisphere MST implant). Three different viral constructs were used: AAV9-CAG-GrabDA2m (n = 13 Area X hemispheres; n = 7 MST hemispheres; WZ Biosciences), AAV9-hSyn-GrabDA1h (n = 5 Area X hemispheres; n = 2 MST hemispheres; Addgene), AAV5-CAG-Dlight1.1 (n = 1 Area X hemisphere; Addgene). During the same surgery, optical fibre or fibres attached to a metal ferrule (Doric, 400 µm core) were inserted above injection sites (Area X: +5.6 A, +1.5 L (relative to lambda), 2.5 V (relative to pial surface); MST: +4.7 A, +0.7 L, 2.9 V; head angle 20°). Data were collected at least eight weeks after surgery to allow for viral expression. Though the auditory processing stream lies in posterior brain regions several millimetres away from implanted fibres (Extended Data Fig. 1c), we acknowledge that implants necessarily cause brain damage and we cannot rule out the possibility that fibres damaged brain regions that may project to VTA, such as the dorsal strip of the striatum[18].

Surgery for electrophysiology

During implant surgeries, birds were anaesthetized with isoflurane and a bipolar stimulation electrode was implanted into Area X at established coordinates (+5.6 A, +1.5 L [relative to lambda], 2.65 V [relative to pial surface]; head angle 20°)[8]. All VTAx neurons in this dataset are from different birds than those reported in[8]. For recording VTAx neurons, custom microdrives carrying an accelerometer, linear actuator, and home-made electrode arrays (5 electrodes, 3-5 MOhms, microprobes.com) were implanted into a region where antidromically identified VTAx neurons were intraoperatively identified (n = 4 birds). For recording VTAother neurons, either custom microdrives as described above (n = 4 birds) or 16-channel movable electrode bundles (Innovative Neurophysiology) were used (n = 3 birds).

Surgery for tracing

For tracing experiments, two adult male birds were used to determine the connectivity between MST and the core, nucleated song system (Extended Data Fig. 1f,g), as well as replicate past results showing MST and Area X-projecting neurons co-localize in VTA but are not co-labelled (Extended Data Fig. 1e)[18]. In three hemispheres, 40 nl of retrograde, fluorescently labelled cholera toxin subunit B (CTB, Molecular Probes) was injected into Area X (+5.6 A, +1.5 L, 2.85 V; head angle 20°) and a different colour CTB was injected into MST (+4.7 A, +0.7 L, 2.9 V; head angle 20°) (Extended Data Fig. 1d). Injections into MST and Area X were made with a Nanoject II (Drummond Scientific).

Water reward task

Birds acclimatized to the homecage for two to three days with ad lib food and water, a mirror, a perch, an inactive water spout and distinct red and white LED lights. During the first phase of training, ad lib water was removed and the reward light cue (0.5 s illumination of red or white LED light; reward light colour varied by bird) was presented with an exponentially distributed, average inter-trial interval of 180 s. At the offset of illumination, 5.0 ± 1.5 µl of water was dispensed from the spout below the reward light with a 100% water reward probability. After birds learned to reliably peck the spout following the reward light cue (greater than 70% retrieval rate), we made water dispensation contingent on spout contact within 8 s of the reward light cue offset. Next we introduced a distinct 0.5 s no-reward light cue of different colour on the opposite side of the homecage from the reward light cue; it did not have a spout underneath, and never resulted in a water reward. Reward and no-reward light cue trials were randomly interleaved and presented at exponentially distributed inter-trial intervals averaging 150 s. Once birds learned to ignore the no-reward cue (less than 10% retrieval rate), while still maintaining a greater than 70% reward cue retrieval rate, head-mounted optical ferrules were attached to a fibre optic cable. Two to three days before optical imaging, the reward light cue water reward probability was changed from 100% to 70%. To test if water retrieval rate was influenced by singing, female presence, and their interactions, we fitted generalized linear mixed models with binomial distribution using the glmmTMB package in R. We then conducted post hoc contrast tests between conditions using the emmeans package in R. P values were corrected for multiple testing using the Tukey method (Fig. 1c and Extended Data Fig. 3c). Note that Figs. 1c and 3c were plotted by bird since retrieval by condition was a measure of the bird's interest in water. Figure 1j,p were plotted by each hemisphere because the relationship between the dopamine signal and retrieval rate is related to the dopamine measurement within sessions and within hemisphere. Also note that data in birds with bilateral implants were not recorded at the same time because birds were connected to a single fibre. Thus data in Fig. 1j,p were plotted as independent measurements.

Syllable-targeted DAF

Postoperative birds were placed in a sound isolation chamber equipped with a microphone and two speakers which provided DAF. To implement targeted DAF, the microphone signal was analysed every 2.5 ms using custom LabVIEW software. Specific syllables were targeted by detecting a unique inter-onset interval (onset time of previous syllable to onset time of target syllable) using the sound amplitude as previously described[8]. The targeted syllable was programmed to be distorted with DAF 50% of the time. DAF was a broadband sound bandpassed at 1.5–8 kHz—the same spectral range of zebra finch song. DAF amplitude was measured with a decibel meter (CEM DT-2 85A) and maintained at less than 90 dB.

Photometry data acquisition and analysis

The 470 nm and 405 nm LEDs (Doric LED Driver and Doric Connectorized LEDs) were modulated sinusoidally at 208.6 and 530.5 Hz respectively using custom LabVIEW code. Excitation signals were passed through minicube filters (Doric Fluorescence MiniCube) to the bird through a commutator (Doric Pigtailed Fiber-optic Rotary Joint). Emission signals were measured using a femtowatt photodetector (Newport, Model 2151) or an integrated 4 port minicube and photodetector (Doric) at 40 kHz (to match microphone sampling rate). Demodulation with custom LabVIEW code produced a 470 nm (dopamine) and a 405 (control) signal which were used to calculate the percentage change of the fractional fluorescence signal ($\Delta F/F$ (%) = 100 × (470−405_fit)/mean[470]). Phasic signals were high-pass filtered (4 Hz butterworth); baseline signals at transitions to singing (Extended Data Fig. 6a–l) and courtship state (Extended Data Fig. 7a–d,f) were low-pass filtered (0.25 Hz butterworth). Hemispheres were excluded if peak fluorescence response across all experiments was less than a z-score of 2 or if fibre placement missed Area X or MST. z-Scored $\Delta F/F$ values were calculated as ($\Delta F/F$ (%) − mean[baseline $\Delta F/F$ (%)])/std[baseline $\Delta F/F$ (%)]; std = standard deviation. Baselines were defined as the one second preceding song target, light cue, or spout contact (Figs. 1–4 and Extended Data Figs. 2, 3, 5, 7 and 9). Here and elsewhere in this Article, for analysis of transitions to singing from not-singing periods, singing onset was defined as the first of a sequence of at least 5 syllables with a maximum intersyllable interval of 0.5 s; singing offset was defined

as the offset of the last syllable of a song sequence followed by at least 0.5 s of silence. Accordingly, a 0.5 s baseline was used to ensure that the baseline not-singing window excluded song syllables (Extended Data Fig. 6). To quantify phasic responses to DAF, female calls, reward cues and knocks, we calculated the mean *z*-scored $\Delta F/F$ in a 0.15–0.3 s window after event onset (Figs. 1–4 and Extended Data Figs. 3, 5, and 9). Due to a wider range of latencies to responses to spout contacts (Extended Data Fig. 2), a 0.17–0.5 s window was used to quantify RPE signals. Latencies for significant phasic signals were analysed and quantified as the interval between event onset and peak (or dip) in the windows specified above (Fig. 4 and Extended Data Figs. 2 and 9). To test for change in baseline dopamine levels at transitions from not-singing to singing (Extended Data Fig. 6), we compared the mean *z*-scored $\Delta F/F$ in the 0–0.5 s window before and after song onsets (or offsets). To test for baseline changes in dopamine release before versus after female appearance (Extended Data Fig. 7), we compared the mean *z*-scored $\Delta F/F$ in the 1 s before her cued arrival to the 1–2 s interval after (to allow for the phasic signal to subside). To test the effects of syllable distortion or rewards, female presence, and their interactions on dopamine release, we used a within-subject two-way ANOVA model with the aov function in *R*. We then conducted post hoc contrast tests between conditions using the emmeans package in *R*. *P* values were corrected for multiple testing using the Tukey method (Figs. 1i,o and 3e,f and Extended Data Figs. 3i,n and 5e,f). Unpaired two-sided Wilcoxon rank sum tests were used to test for significance across different groups of hemispheres (Figs. 2e–g and 4e–g and Extended Data Figs. 2e,f, 7e and 9e,j,k,p,q). Paired two-sided Wilcoxon signed rank tests were used to test for significance across the same hemispheres (Figs. 3g and 4e and Extended Data Figs. 2e, 5g, 6e,f,k,l,q,r and 9e,j,p). We used a one-sample *t*-test to compare baseline dopamine levels before and after female appearance (Extended Data Fig. 7f).

Electrophysiology data acquisition and analysis

For the custom microdrives, neural signals were band-pass filtered (0.25–15 kHz) in home-made analogue circuits and acquired at 40 kHz using custom Matlab software. For the 16-channel movable electrode bundles (Innovative Neurophysiology), neural recordings were obtained using 16-channel INTAN headstages with the accompanying recording controller and INTAN acquisition software at a sampling rate of 20 kHz. Single units were identified as VTAx by antidromic identification (stimulation intensities 50-400 μA, 200 μs on the bipolar stimulation electrode in Area X), as previously described[8]. Neurons not identified as projecting to Area X were defined as VTAother neurons. Spike sorting was performed offline using custom MATLAB software. Instantaneous firing rates were defined at each time point as the inverse of the enclosed interspike interval (ISI). Firing rate histograms were constructed with 25-ms bins and smoothed with a 3-bin moving average. To calculate the mean rate and median ISI during singing (Extended Data Fig. 8), the firing rate and median ISI were averaged over all song motifs, with a time-window extending 50 ms before motif onset to 50 ms after motif-offset. The coefficient of variation of the ISI and the peak of the spike-train autocorrelation (STA) in Extended Data Fig. 8 were computed over the entire singing bouts. To test for error responses, we compared the firing activity between randomly interleaved undistorted and distorted song renditions. We computed the *z*-scored difference between the target time-aligned distorted and undistorted firing rate histograms (Extended Data Fig. 4). The target time was defined as the median DAF onset time relative to the distorted syllable onset time. The error response was defined as the mean *z*-scored difference in a 50–125 ms window following target time[8]. To calculate the significance bars shown in Extended Data Fig. 4, spiking activity within ±1 s relative to target onset was binned in a moving window of 30 ms with a step size of 2 ms. Each bin after the target time was tested against all the bins in the previous 1 s (the prior) using a *z*-test[8]. To test the effects of syllable distortion, female presence, and their interactions on dopamine spiking, we used a within-subject two-way ANOVA model with the aov function in R. We then conducted post hoc contrast tests between conditions using the emmeans package in R. *P* values were corrected for multiple testing using the Tukey method (Extended Data Fig. 4e,f). A paired two-sided Wilcoxon signed rank test was used to test for significance in Extended Data Figs. 4g, 6w,x and 8.

Courtship interactions

Experiments were performed in the male's homecage in a sound isolation chamber. During electrophysiological recording sessions, spiking data were first collected when the male was singing alone for at least 35 song motifs before the female was introduced. For fibre photometry experiments where we examined dopamine release at the transition to courtship state (Extended Data Fig. 7), we controlled for the precise moment of perceived female arrival by playing two female calls through speakers immediately prior to presenting the female. In all experiments, the female cage was placed next to the male's within the sound isolation chamber allowing birds to hear and see each other.

Reporting summary

Further information on research design is available in the Nature Portfolio Reporting Summary linked to this article.

Data availability

The data that support the findings of this study are available at https://osf.io/dcugn/. Source data are provided with this paper.

Code availability

The data collection and analysis code used for this study are available at https://osf.io/dcugn/.

Acknowledgements The authors thank A. Mohebi, N. Uchida, B. Ito and members of the Goldberg laboratory for comments; A. Raha for artwork; Z. Zhao for statistical advice; and A. Enzerink and A. Podury for technical assistance. V.G. was supported by a Simons Foundation Postdoctoral Fellowship and a NIH/NINDS Pathway to Independence Award (grant no. K99/R00NS102520), P.A.P. was supported by NIH/NINDS (grant no. F32NS098634), and J.H.G. was supported by NIH/NINDS (grant no. R01NS094667).

Author contributions A.R., V.G. and J.H.G. designed the research, analysed data and wrote the paper. A.R., V.G., A.D., P.A.P. and B.K. performed experiments.

Competing interests The authors declare no competing interests.

Additional information

Supplementary information The online version contains supplementary material available at https://doi.org/10.1038/s41586-023-06580-w.

Correspondence and requests for materials should be addressed to Vikram Gadagkar or Jesse H. Goldberg.

Peer review information *Nature* thanks the anonymous reviewer(s) for their contribution to the peer review of this work. Peer review reports are available.

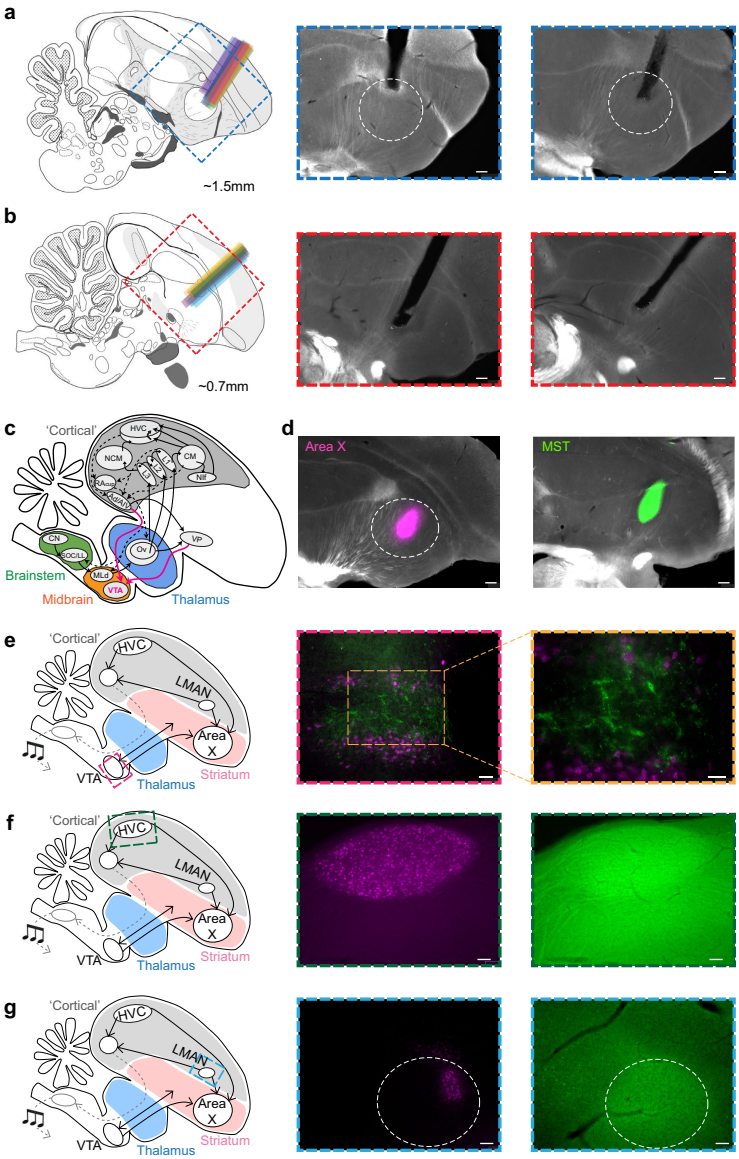

Extended Data Fig. 1 | Histological verification of fiber placement in Area X and MST. a, Left: Locations of all Area X fiber implants ($n = 19$ hemispheres), implanted 1.5 mm lateral to midline. Right: sagittal slices of two hemispheres (Area X, white circle). Scale bars: 250 um. Left: Schematic from the ZEBrA database (http://www.zebrafinchatlas.org)[20]. **b**, Sites of MST fibers ($n = 9$ hemispheres), implanted 0.7 mm lateral to midline and 1 mm posterior to the Area X implant. Left: Schematic from the ZEBrA database (http://www.zebrafinchatlas.org)[20]. Right: sagittal slices of two MST hemispheres. Scale bars: 250 um. **c**, Schematic of the songbird auditory system, including forebrain projections to VTA from dorsal arcopallium (AD), ventral intermediate arcopallium (AIV), and ventral pallidum (VP). Schematic adapted from[19,22,23,29]. Note that Area X and MST fibers were several millimeters anterior this auditory pathway. **d**, Injection sites of the retrograde tracer cholera toxin beta subunit (CTB) into Area X (left, magenta) and MST (right, green) into the same hemisphere (independently repeated in $n = 3$ hemispheres; $n = 2$ birds; Methods). Scale bars: 250 um. **e**, Zebra finch brain schematic with pink rectangle around VTA (left). MST and Area X projecting neurons co-localize in VTA but are not co-labeled, consistent with previous findings (middle)[18]. Expanded view at right. Scale bars: 75 um (middle) and 50 um (right). **f-g**, Core nuclei of the song system project to Area X, but not MST (independently repeated in $n = 3$ hemispheres; $n = 2$ birds). **f**, Schematic of zebra finch brain, with green rectangle surrounding HVC (left). HVC contains Area X projecting neurons (magenta, middle), but no MST projecting neurons in the same hemisphere (right, green), consistent with past work[18]. Scale bars: 75 um. **g**, Schematic of zebra finch brain, with blue rectangle surrounding LMANcore (left). LMANcore contains Area X projecting neurons (magenta, middle), but no MST projecting neurons in the same hemisphere (right, green), consistent with past work[18,19] (middle and right; approximate boundary of LMANcore denoted by white circle). Scale bars: 75 um.

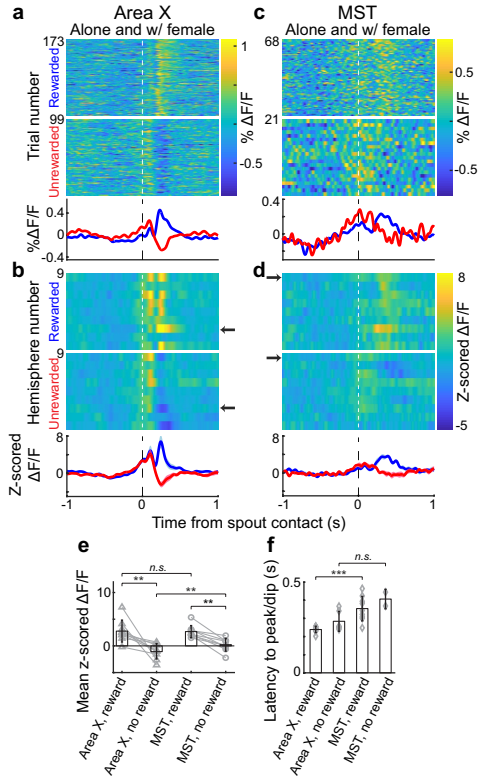

Extended Data Fig. 2 | Reward prediction error signals exist in Area X and MST. a, Single trial DA responses from one Area X hemisphere in response to a water reward (top) or reward omission (bottom), aligned to spout contacts following 'reward' light cues. **b**, Average z-scored ΔF/F signals across 9 Area X hemispheres, example hemisphere in **a** indicated by black arrow (top), average across all hemispheres (mean ± SEM; bottom). **c-d**, Data plotted as in **a-b** for 9 MST hemispheres. **e**–**f**, Reward signals were larger and faster in Area X compared to MST. **e**, Scatterplots showing average values across all 9 Area X and 9 MST hemispheres (mean ± SD, black) and mean z-scored values for each hemisphere (gray) for reward and reward omission in the 170-500 ms window following spout contact (Area X, reward vs. Area X, no reward: P = 0.0039; Area X, reward vs. MST, reward: P = 1; MST, reward vs. MST, no reward: P = 0.0039; Area X, no reward vs. MST, no reward: P = 0.063; paired, two-sided Wilcoxon signed rank test). **f**, Latency to peak (rewarded trials) or dip (omission trials) of the z-scored response in the 170–500 ms window after spout contact (mean ± SD, black; single hemispheres, gray; only responses that were greater than a z-score value of 2 within the window were included; Area X, reward vs MST, reward: P = 0.00033; Area X, no reward vs MST, no reward: P = 0.071; unpaired, two-sided Wilcoxon rank sum test). ** $P < 0.01$, *** $P < 0.001$, *n.s.* not significant.

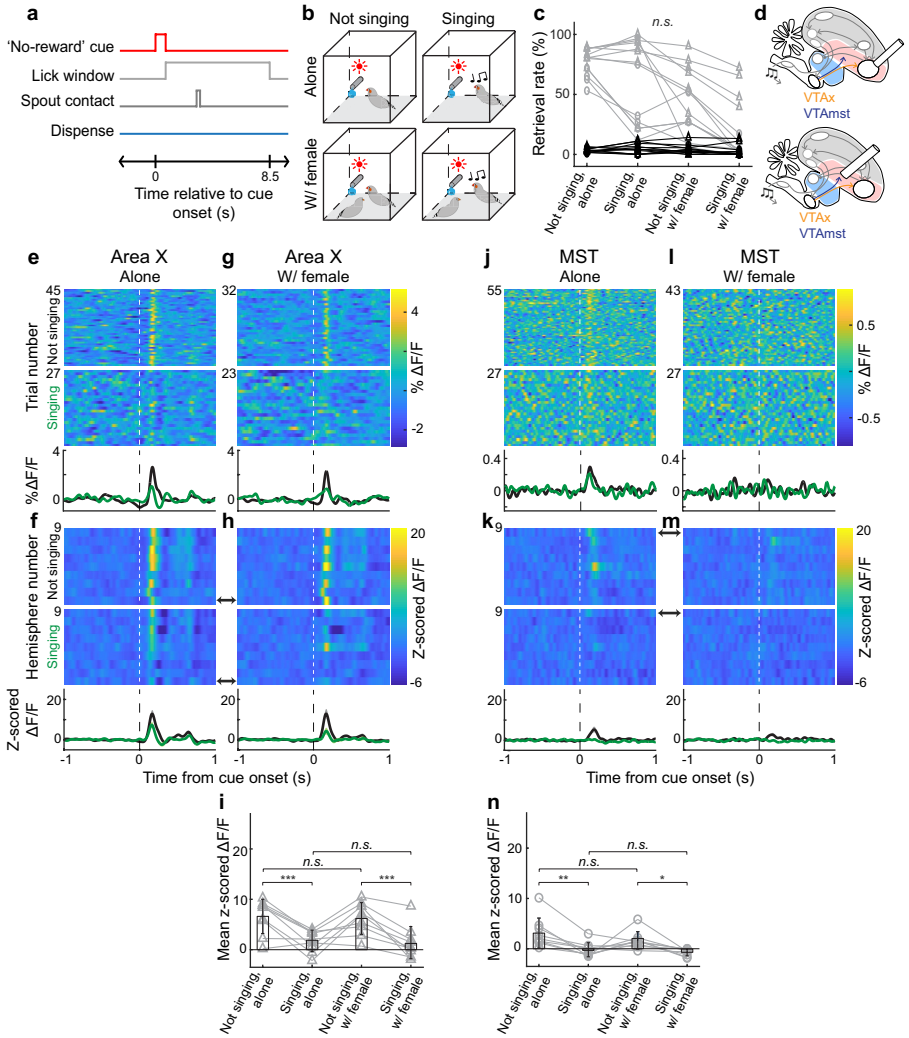

Extended Data Fig. 3 | Singing reduces dopaminergic responses to 'no-reward' light cues in both Area X and MST. a, Example 'no-reward' light cue trial. **b**, Water availability under four behavioral conditions. **c**, Water retrieval probability for 'no-reward' (black) and 'reward' (gray) light cues across behavioral conditions (Area X implanted bird: triangles; MST implanted bird: circles; *n.s.*; generalized linear mixed effects model with post-hoc contrast tests; Methods). **d**, Brain schematics showing recording sites. **e-f**, DA responses in Area X to the 'no-reward' light when the bird was alone. **e**, DA responses for single trials from a single Area X hemisphere during not singing (top) or singing (bottom) conditions. **f**, Average z-scored ΔF/F signals across 9 Area X hemispheres, example hemisphere in **e** indicated by black arrow (top), average across all hemispheres (mean ± SEM; bottom). **g-h**, Data plotted as in **e-f** when in the presence of a female. **i**, Average values across all Area X hemispheres (mean ± SD, black) and mean z-scored values for each hemisphere (gray; $n = 9$ Area X hemispheres) for the four behavioral conditions in **e**–**h** (not singing, alone vs singing, alone: P = 0.00051; not singing, alone vs. not singing, with female: P = 0.98; singing, alone vs. singing with female: P = 0.99; not singing, with female vs. singing, with female: P = 0.00060; 2-way ANOVA and post-hoc Tukey; Methods). **j**–**n**, Data plotted as in **e-i** for DA recordings in 9 MST hemispheres. **n**, Average values across all MST hemispheres (mean ± SD, black) and mean z-scored values for each hemisphere ($n = 9$ hemispheres; gray) for the four behavioral conditions in **j**–**m** (not singing, alone vs singing, alone: P = 0.0015; not singing, alone vs. not singing, with female: P = 0.27; singing, alone vs. singing, with female: P = 0.91; not singing, with female vs. singing, with female: P = 0.025; 2-way ANOVA and post-hoc Tukey; Methods). * $P < 0.05$, ** $P < 0.01$, *** $P < 0.001$, *n.s.* not significant.

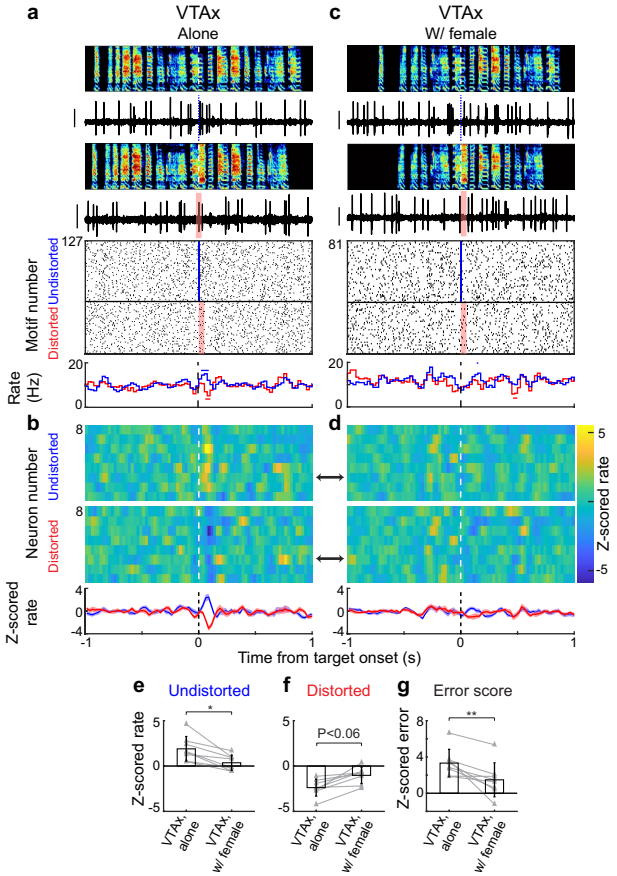

Extended Data Fig. 4 | Modulation of singing-related error signals during courtship is also observed at the level of VTAx spikes. a, Spectrograms, single trial spiking activity, and raster plots for undistorted (top) and distorted (bottom) renditions recorded in a single antidromically identified VTAx neuron of a bird singing alone, plotted above firing rate histograms (plots aligned to target onset; blue: undistorted; red: distorted). **b**, Z-scored average from 8 antidromically identified VTAx neurons aligned to undistorted (top) and distorted (bottom) renditions, black arrow indicates example neuron shown in **a**; bottom: average z-scored response (mean ± SEM). **c**, Data plotted as in **a** for the same VTAx neuron recorded during courtship singing. **d**, Data plotted as in **b** for the same VTAx neurons recorded during courtship singing. **e-f**, Scatter plots (gray, $n = 8$ neurons) and mean ± SD (black) of average z-scored firing rate in the 50–125 ms following undistorted (**e**; P = 0.026; 2-way ANOVA and post-hoc Tukey; Methods) and distorted (**f**; P = 0.056; 2-way ANOVA and post-hoc Tukey; Methods) renditions during alone versus female directed singing across all VTAx neurons. **g**, Z-scored error responses for each neuron (gray; $n = 8$) and mean ± SD (black) when birds sang alone versus to females (P = 0.008; paired, two-sided Wilcoxon signed rank test). Horizontal bars in histograms (**a, c**) indicate significant deviations from baseline, $P < 0.05$ for a one-sided z test. Scale bars in **a** and **c** for spiking activity is 1 mV. * $P < 0.05$, ** $P < 0.01$.

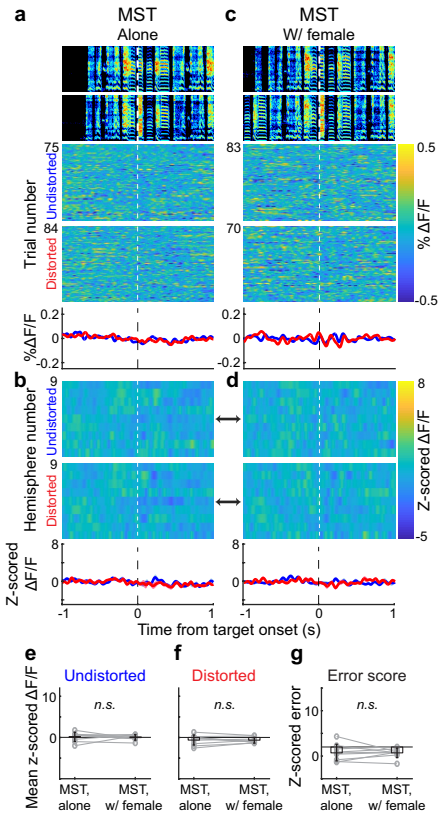

Extended Data Fig. 5 | Singing-related performance error signals are not observed in MST during courtship singing. a, Spectrograms and single trial DA responses for undistorted (top) and distorted (bottom) renditions recorded in a single MST hemisphere of a bird singing alone, plotted above average ΔF/F signals (different hemisphere from Fig. 2c; plots aligned to target onset; blue: undistorted; red: distorted). **b**, Z-scored average from 9 MST hemispheres aligned to undistorted (top) and distorted (bottom) renditions, black arrow indicates example hemisphere shown in **a**; bottom: average z-scored response (mean ± SEM). **c**, Data plotted as in **a** for the same hemisphere measured during courtship singing. **d**, Data plotted as in **b** for the same hemispheres recorded during courtship singing. **e-f**, Scatter plots of average across all hemispheres (mean ± SD, black) and mean z-scored ΔF/F value for each hemisphere (gray) in the 150–300 ms following undistorted (**e**) and distorted (**f**) renditions in MST during alone versus female directed singing. **g**, Z-scored error responses when birds sang alone versus to females (mean ± SD, black; single hemispheres, gray). *n.s.* not significant for a 2-way ANOVA and post-hoc Tukey (**e** and **f**; Methods) and for a paired two-sided Wilcoxon signed rank test (**g**); $n = 9$ MST hemispheres.

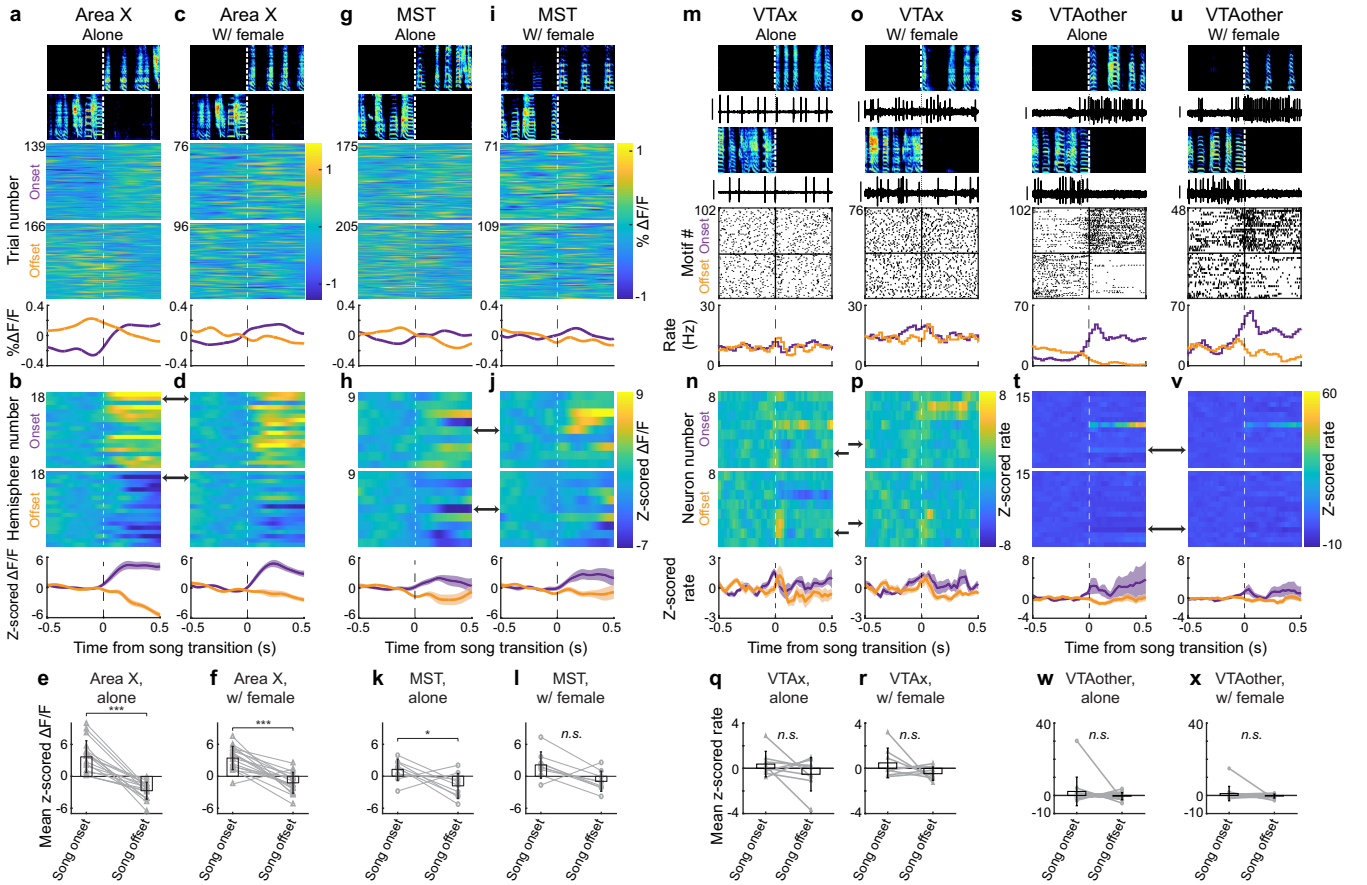

Extended Data Fig. 6 | Baseline levels of DA release, but not VTA spiking, increase during both alone and female directed singing. a, Spectrograms and single trial DA signals for song onsets (top) and offsets (bottom) recorded in a single Area X hemisphere of a bird singing alone, plotted above average ΔF/F signals (purple and orange aligned to song onset or offset, respectively). **b**, Z-scored average from 18 Area X hemispheres aligned to song onsets (top) and offsets (bottom), black arrow indicates example hemisphere from **a**; bottom: average z-scored signals (mean ± SEM). **c-d**, Data plotted as in **a-b** for the same hemisphere measured during courtship singing. **e-f**, Mean z-scored ΔF/F value for each Area X hemisphere (gray) in the 0-500 ms window following song onset and offset during alone (**e**; P = 2.0E-4; paired, two-sided Wilcoxon signed rank test) and female directed singing (**f**; P = 3.9E-4; paired, two-sided Wilcoxon signed rank test) (black: mean ± SD across all hemispheres). **g–l**, Data plotted as in **a–f** for 9 MST hemispheres. **k**, P = 0.039; paired, two-sided Wilcoxon signed rank test. **m**, Spectrograms, single trial spiking activity, and raster plots for song onset (top) and offset (bottom) recorded in a single VTAx neuron of a bird singing alone, plotted above firing rate histograms (plots aligned to song onset or offset). **n**, Z-scored firing rate histograms from 8 VTAx neurons aligned to song onset (top) and offset (bottom), black arrow indicates example neuron shown in **m**; bottom: average z-scored firing rate (mean ± SEM). **o-p**, Data plotted as in **m-n** for the same VTAx neurons recorded during courtship singing. **q-r**, Scatter plots (gray) and mean ± SD (black) of average z-scored firing rate in the 0-500 ms window following song onset and offset during alone (**q**) and female directed singing (**r**) across all VTAx neurons. **s–x**, Data plotted as in **m–r** for VTAother neurons. Scale bars in **m, s** and **u** for spiking activity is 1 mV, and for **o** is 0.25 mV. * $P < 0.05$, *** $P < 0.001$, *n.s.* not significant for a paired two-sided Wilcoxon signed rank test; $n = 18$ Area X and $n = 9$ MST hemispheres (**e,f,k,l**) and $n = 8$ VTAx and $n = 14$ VTAother neurons (**q,r,w,x**).

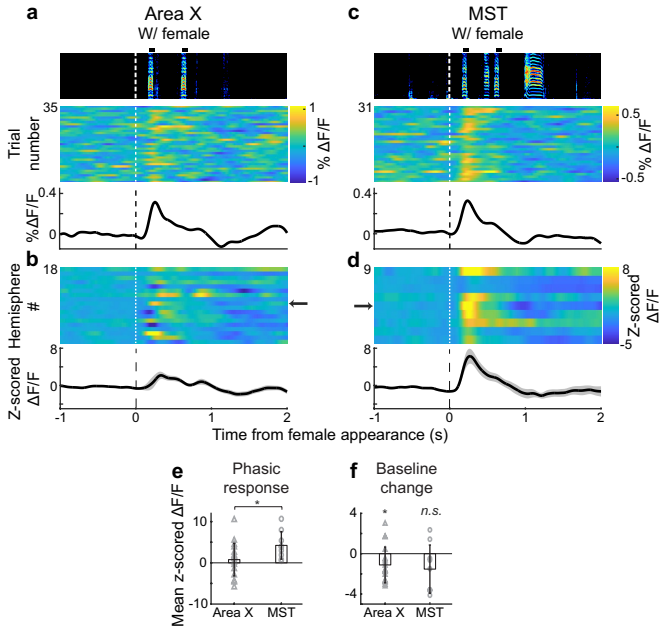

Extended Data Fig. 7 | The cued moment of female appearance evokes phasic, but not sustained, activation of DA release. a, Spectrogram and single trial Area X DA responses to female appearance during the transition between alone and with-female conditions, plotted above average ΔF/F signals (plots aligned to onset of female call playback). Black boxes above spectrogram indicate female call playbacks. **b**, Z-scored average from 18 Area X hemispheres, black arrow indicates example hemisphere shown in **a**; bottom: average z-scored response (mean ± SEM). **c**-**d**, Data plotted as in **a**-**b** for DA signals recorded in 9 MST hemispheres. **e**, Scatter plots showing phasic response across all hemispheres (mean ± SD, black) and mean z-scored ΔF/F value for each hemisphere (gray; Area X: $n = 18$ and MST: $n = 9$ hemispheres) in the 150–300 ms window following female call onset cueing female appearance (triangles: Area X; circles: MST; P = 0.029; unpaired, two-sided Wilcoxon rank sum test). **f**, Scatter plots of baseline change across all hemispheres (mean ± SD, black) and mean z-scored ΔF/F value for each hemisphere (gray) in the 1–2 s window following cued female appearance (triangles: Area X; circles: MST; Methods; Area X: P = 0.017; MST: P = 0.097; one-sample t test). *$P < 0.05$, *n.s.* not significant.

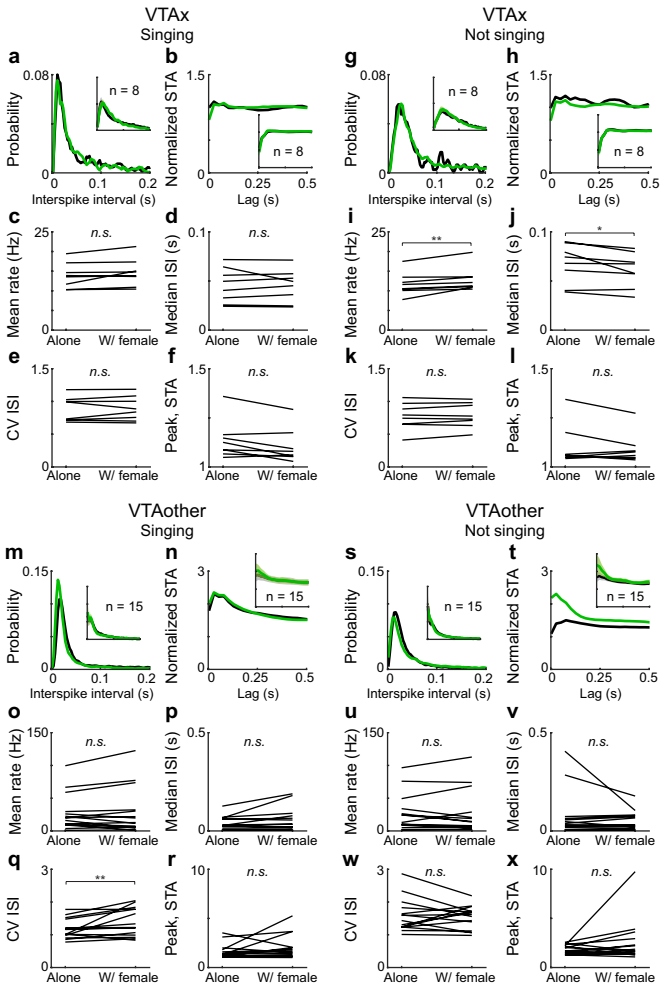

Extended Data Fig. 8 | Discharge statistics of VTAx DA neurons do not depend on courtship context during singing and were subtly affected during not-singing periods. a-b, ISI distribution (**a**) and normalized spike train autocorrelogram (STA) (**b**) during singing alone (black) and female directed (green) song for a single VTAx neuron. Insets: mean ± SEM for 8 VTAx neurons. **c-f**, Mean firing rate (**c**), median ISI (**d**), coefficient of variation of the ISI distribution (CV ISI; **e**), and peak of the STA (**f**) for 8 VTAx neurons recorded when males sang alone and sang female-directed song. **g**–**l**, Data plotted as in **a-f** for the same 8 VTAx neurons during not singing periods. **i**, P = 0.008; paired, two-sided Wilcoxon signed rank test. **j**, P = 0.02; paired, two-sided Wilcoxon signed rank test. **m**–**x**, Data plotted as in **a**–**l** for 15 VTAother neurons (Methods). **q**, P = 0.005; paired, two-sided Wilcoxon signed rank test. * $P < 0.05$, ** $P < 0.01$, n.s not significant for a paired two-sided Wilcoxon signed rank test.

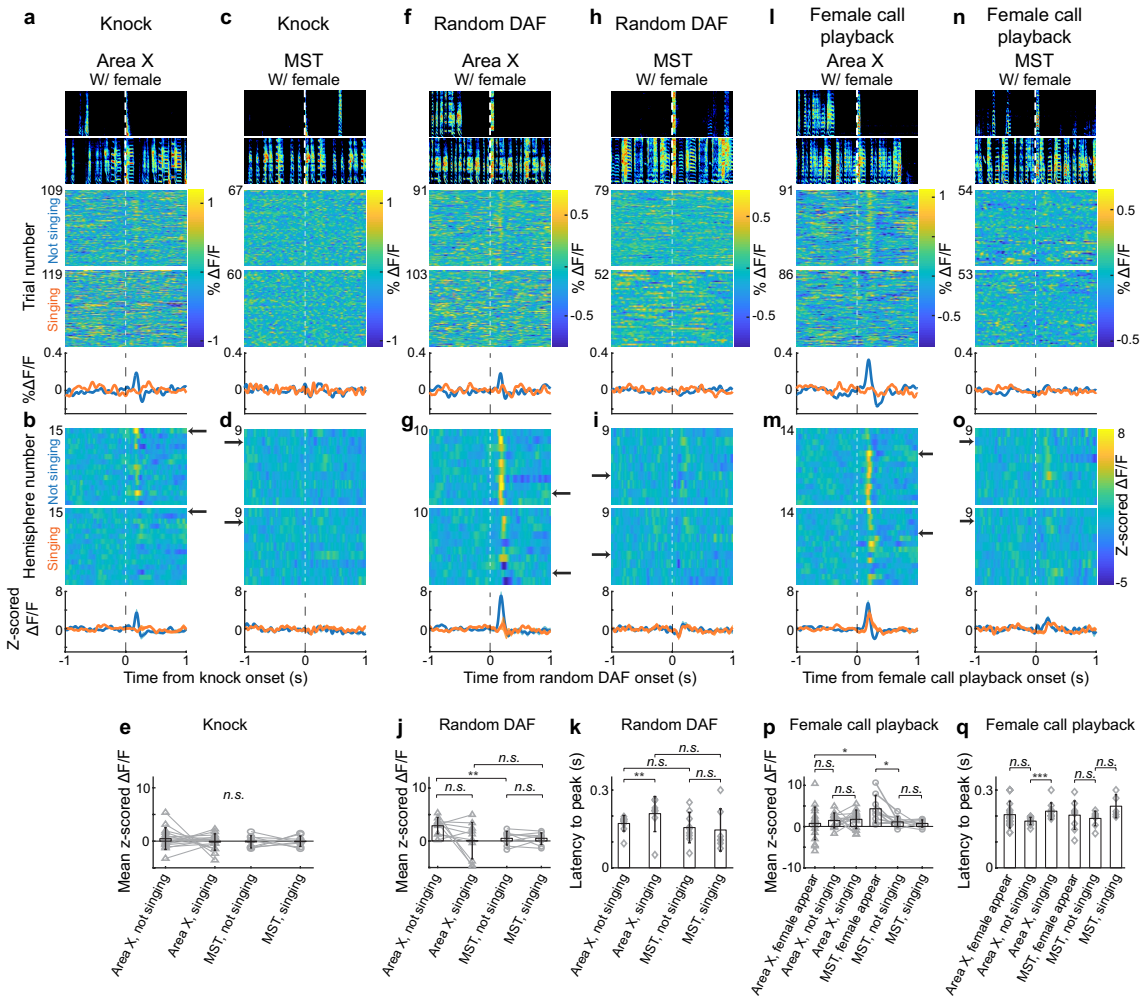

Extended Data Fig. 9 | Socially irrelevant sounds and pre-recorded female calls played during courtship do not drive reliable DA responses. **a**–**e**, Knock responses. **a**, Spectrograms and single trial Area X DA responses to knock sounds played during not-singing (top) or singing (bottom) periods of the courtship interaction, plotted above average ΔF/F signals (plots aligned to onset of knock) in a single hemisphere. **b**, Z-scored average from 15 Area X hemispheres, black arrow indicates example hemisphere shown in **a**; bottom: average z-scored response (mean ± SEM). **c**-**d**, Data plotted as in **a**-**b** for knock responses recorded in MST. **e**, Mean z-scored ΔF/F values in the 0.15–0.3 s window following the onset of knock sounds in Area X and MST during singing and not-singing periods (gray, single hemispheres; black, mean ± SD across hemispheres; triangles: Area X; circles: MST). **f**–**k**, Random DAF responses. **f**–**j**, Data plotted as in **a**–**e** for Area X and MST responses to the sound of DAF played randomly throughout the courtship interaction, including during singing and not-singing periods (Area X: $n = 10$; MST: $n = 9$ hemispheres). **j**, Area X, not singing vs. MST, not singing: P = 0.0041; unpaired, two-sided Wilcoxon rank sum test. **k**, Latencies to peak responses to random DAF (gray, single hemispheres; black, mean ± SD across hemispheres; Methods; Area X, not singing vs. Area X, singing: P = 0.0085; paired, two-sided Wilcoxon signed rank test). **l**–**q**, Pre-recorded female calls. Data plotted as in **f**–**k** for Area X and MST responses to the sound of pre-recorded female calls played through a speaker at random times throughout a live courtship interaction, including during singing and not-singing periods (Area X: $n = 14$; MST: $n = 9$ hemispheres). Note that playback of these calls did not evoke reliable DA responses in Area X or MST during song. **p**, Area X, female appear vs. MST, female appear: P = 0.029; unpaired two-sided Wilcoxon rank sum test; MST, female appear vs. MST, not singing: P = 0.040; paired two-sided Wilcoxon signed rank test). **q**, Area X, not singing vs. Area X, singing: P = 3.6E-4; paired two-sided Wilcoxon signed rank test). * $P < 0.05$, ** $P < 0.01$, *** $P < 0.001$, *n.s.* not significant for a paired two-sided Wilcoxon signed rank test (within Area X and within MST **e,j,p**) and for an unpaired two-sided Wilcoxon rank sum test (**k,q**; across Area X and MST in **e,j,p**).

nature portfolio

Corresponding author(s): Jesse H. Goldberg, Vikram Gadagkar

Last updated by author(s): Jul 12, 2023

Reporting Summary

Nature Portfolio wishes to improve the reproducibility of the work that we publish. This form provides structure for consistency and transparency in reporting. For further information on Nature Portfolio policies, see our Editorial Policies and the Editorial Policy Checklist.

Statistics

For all statistical analyses, confirm that the following items are present in the figure legend, table legend, main text, or Methods section.

n/a	Confirmed
☐	☒ The exact sample size (*n*) for each experimental group/condition, given as a discrete number and unit of measurement
☐	☒ A statement on whether measurements were taken from distinct samples or whether the same sample was measured repeatedly
☐	☒ The statistical test(s) used AND whether they are one- or two-sided *Only common tests should be described solely by name; describe more complex techniques in the Methods section.*
☐	☒ A description of all covariates tested
☐	☒ A description of any assumptions or corrections, such as tests of normality and adjustment for multiple comparisons
☐	☒ A full description of the statistical parameters including central tendency (e.g. means) or other basic estimates (e.g. regression coefficient) AND variation (e.g. standard deviation) or associated estimates of uncertainty (e.g. confidence intervals)
☐	☒ For null hypothesis testing, the test statistic (e.g. *F*, *t*, *r*) with confidence intervals, effect sizes, degrees of freedom and *P* value noted *Give P values as exact values whenever suitable.*
☒	☐ For Bayesian analysis, information on the choice of priors and Markov chain Monte Carlo settings
☒	☐ For hierarchical and complex designs, identification of the appropriate level for tests and full reporting of outcomes
☒	☐ Estimates of effect sizes (e.g. Cohen's *d*, Pearson's *r*), indicating how they were calculated

Our web collection on statistics for biologists contains articles on many of the points above.

Software and code

Policy information about availability of computer code

Data collection	Photometry data were collected using Labview 2015 (see Code Availability Statement) and electrophysiology data were collected using Matlab 2014 and Intan Data Acquisition Software.
Data analysis	Data were analyzed using custom code written in Matlab 2019a (see Code Availability Statement).

For manuscripts utilizing custom algorithms or software that are central to the research but not yet described in published literature, software must be made available to editors and reviewers. We strongly encourage code deposition in a community repository (e.g. GitHub). See the Nature Portfolio guidelines for submitting code & software for further information.

Data

Policy information about availability of data

All manuscripts must include a data availability statement. This statement should provide the following information, where applicable:

- Accession codes, unique identifiers, or web links for publicly available datasets
- A description of any restrictions on data availability
- For clinical datasets or third party data, please ensure that the statement adheres to our policy

The data that support the findings of this study are available at https://osf.io/dcugn/. Please contact the corresponding authors with any further questions.

Field-specific reporting

Please select the one below that is the best fit for your research. If you are not sure, read the appropriate sections before making your selection.

☒ Life sciences ☐ Behavioural & social sciences ☐ Ecological, evolutionary & environmental sciences

For a reference copy of the document with all sections, see nature.com/documents/nr-reporting-summary-flat.pdf

Life sciences study design

All studies must disclose on these points even when the disclosure is negative.

Sample size	No statistical methods were used to determine sample size. We used a minimum of 8 neurons/birds/brain hemispheres per condition and experiment. Sample sizes used in this study are comparable to or exceed the typical sample sizes used in the field, e.g. Hisey et al. A common neural circuit mechanism for internally guided and externally reinforced forms of motor learning. Nature Neuroscience 21, 589-597 (2018) https://doi.org/10.1038/s41593-018-0092-6 Tanaka et al. A mesocortical dopamine circuit enables the cultural transmission of vocal behaviour. Nature 563, 117-120 (2018) https://doi.org/10.1038/s41586-018-0636-7
Data exclusions	No data were excluded.
Replication	All reported differences in electrophysiology and photometry experiments were replicated in a minimum of 8 neurons/birds/brain hemispheres in independent sessions. Histological verification was replicated in a minimum of 3 brain hemispheres in independent experiments.
Randomization	Animals were randomly allocated into the experimental groups. Trial types were psedo-randomly determined by a computer program in real time.
Blinding	The investigators were not blinded to allocation during experiments and outcome assessment. All experiments had within-animal controls and blinding was not necessary. Data collection was automated to exclude experimenter bias and experimenters were blinded to experimental conditions during sorting of waveforms into single neurons.

Reporting for specific materials, systems and methods

We require information from authors about some types of materials, experimental systems and methods used in many studies. Here, indicate whether each material, system or method listed is relevant to your study. If you are not sure if a list item applies to your research, read the appropriate section before selecting a response.

Materials & experimental systems

n/a	Involved in the study
☒	☐ Antibodies
☒	☐ Eukaryotic cell lines
☒	☐ Palaeontology and archaeology
☐	☒ Animals and other organisms
☒	☐ Human research participants
☒	☐ Clinical data
☒	☐ Dual use research of concern

Methods

n/a	Involved in the study
☒	☐ ChIP-seq
☒	☐ Flow cytometry
☒	☐ MRI-based neuroimaging

Animals and other organisms

Policy information about studies involving animals; ARRIVE guidelines recommended for reporting animal research

Laboratory animals	Zebra Finches
Wild animals	No wild animals were used in this study.
Field-collected samples	No field-collected samples were used in this study.
Ethics oversight	All experiments were carried out in accordance with NIH guidelines and were approved by the Cornell Institutional Animal Care and Use Committee.

Note that full information on the approval of the study protocol must also be provided in the manuscript.